Struct Multidisc Optim (2009) 37:351–366
DOI 10.1007/s00158-008-0242-7

RESEARCH PAPER

Optimal design of adaptive structures Part II. Adaptation to impact loads

Marcin Wiklo · Jan Holnicki-Szulc

Received: 3 August 2007 / Revised: 18 October 2007 / Accepted: 23 January 2008 / Published online: 8 April 2008

Abstract This paper is a continuation of the article entitled "Remodeling for Impact Reception." It presents a generalization of the previously discussed concept on optimal remodeling of elasto-plastic structures exposed to impact load, where remodeling process is simulated via *virtual distortion method* (VDM). The resultant stiffest structure determined in the first part of this paper determines the initial configuration to design the optimal adaptive structure. It is assumed that considered structure can be equipped with so-called structural fuses with plastic-like behavior and controllable yield stress levels. Such an adaptive structure can still be optimized by the proper selection of locations for structural fuses and by the proper tuning of yield stress levels to the identified impact load. Maximization of the impact energy dissipation as the objective function allows significant reduction of residual vibrations after a few milliseconds. VDM-based algorithms for fast, complex reanalysis of dynamically loaded elasto-plastic structures and their sensitivity analysis are the key tools for the above-mentioned optimization procedures.

M. Wiklo (✉)
Institute of Applied Mechanics,
Technical University of Radom,
Radom, Poland
e-mail: mwiklo@ippt.gov.pl, marcin.wiklo@pr.random.pl

M. Wiklo · J. Holnicki-Szulc
Institute of Fundamental Technological Research,
Warsaw, Poland

J. Holnicki-Szulc
e-mail: holnicki@ippt.gov.pl

Keywords Fast structural reanalysis · Virtual distortion method · Adaptive impact absorption · Optimal design · Impact loads

1 Nomenclature

AIA	adaptive impact absorbtion
VDM	virtual distortion method
IVDM	impulse virtual distortion method
IVFM	impulse virtual force method
MR-fluid	magneto rheological fluid (MRF)

2 Introduction

The first part of this paper (Wiklo and Holnicki-Szulc 2008) was devoted to the presentation of a numerical tool effective for the simulation of structural modifications and to its application to maximization of structural stiffness. Having the total material volume and the external impact load (eventually several load states) defined, the objective was to find such material redistribution that an average structural response measured in displacements is minimized. The numerical tool allowing effective solution of this problem was based on the gradient optimization approach making use of versions of the so-called *virtual distortion method* (VDM).

The second part presented below deals with the generalization for nonlinear structural responses, with piece-wise linear, plastic-like behavior of elements, simulating properties of actively controlled adaptive structures. It is assumed that the overall effect of elasto-plastic response to impact loads can be achieved installing *structural fuses* with controllable plastic levels. In this way, optimally controlled *adaptive structures*

can simulate the response of hypothetic elasto-plastic structures with their plastic stresses tuned optimally to on-line identified impact loads. Controllable dissipaters based on magneto rheological fluids or piezo-valves can play the role of such structural fuses (Holnicki-Szulc et al. 2003). Another technological challenge is determined by the problem of real-time impact load identification (Sekua et al. 2006).

The first three sections of this paper are dedicated to the further development of the VDM-based numerical tool for fast structural modifications under dynamic loads. The main generalization of the approach presented in the first part of this paper is due to physical nonlinearity taken into account and the coupled problem including simultaneous geometric and physical modifications. The final section is devoted to application of this numerical tool to the design of optimal adaptive structures.

3 Modelling of material nonlinearities (modification of $\sigma^\star$)

The equation of motion for elasto-plastic structures modelled via *virtual distortions* (plastic distortions) takes the following form (Wiklo and Holnicki-Szulc 2008):

$$M_{NM}\ddot{u}_M(t) + G_{Ni}^T S_{ij}\left[G_{jM}u_M(t) - l_{\underline{j}}\beta^0_{\underline{j}}(t)\right] = f_N(t) \quad (1)$$

or, alternatively,

$$M_{NM}\ddot{u}_M(t) + G_{Ni}^T S_{ij}\left[l_{\underline{j}}\left(\varepsilon_{\underline{j}}(t) - \beta^0_{\underline{j}}(t)\right)\right] = f_N(t) \quad (2)$$

which expresses displacements through strains, correlated via the following relation:

$$l_{\underline{i}}\varepsilon_{\underline{i}}(t) = G_{iM}u_M(t) \quad (3)$$

where G_{iM} is a transformation matrix, whose elements are related to cosines of angles between elements and directions of degrees of freedom; S_{ij} is a diagonal matrix with elements over diagonal $S_{ii} = E_{\underline{i}}A_{\underline{i}}/l_{\underline{i}}$; E_i, the Young's modulus; A_i, the cross section; and l_i, the length of an element i.

The summation over time in subsequent equations indicates the time period, discretized into a finite number of time instances $\langle 0, 1, \ldots, t, \ldots, T\rangle$. The time integration of the equation of motion was performed by the Newmark scheme. Except for the initial condition at $t = 0$, all other quantities are calculated starting from the first time step onwards. Therefore, to be consistent with the numerical integration procedure, the summation in subsequent equations starts from $t = 1$ and finishes at $t = T$.

The structural response can be superimposed from the elastic part and the component due to plastic distortions:

$$u_N(t) = u_N^L(t) + \sum_{\tau\le t} B^{\varepsilon}_{Nk}(t+1-\tau)\beta^0_k(\tau) \quad (4)$$

where the vector $u_N^L(t)$ denotes the development of displacements in degrees of freedom N, determined for the elastic structure, while $\beta^0_k(t)$ denotes *virtual distortions* simulating plastic yielding of the element. Index N is related to all degrees of freedom of the structure while index k is related only to plastified elements. B^{ε}_{Nk} denotes a dynamic *influence matrix* containing the displacement history induced in the N-th degree of freedom as response to the unitary distortion impulse applied to the k-th element. The impulse is applied as a Dirac-like function in the form of a pair of balanced forces causing unitary deformation.

The strain development $\varepsilon(t)$ can be obtained from the formula (4) after multiplying it by the quantity $\frac{1}{L_{\underline{i}}}G_{\underline{i}N}$:

$$\varepsilon_i(t) = \varepsilon_i^L(t) + \sum_{\tau\le t} D^{\varepsilon}_{ik}(t+1-\tau)\beta^0_k(\tau) \quad (5)$$

where the vector $\varepsilon_i^L(t)$ denotes the strain development in the elastic structure and D^{ε}_{ik} denotes the dynamic influence matrix describing the strain evolution in element i, in the time step t in response to a unitary impulse of *virtual distortion* generated in the time step τ in the element k.

The stress development takes the form:

$$\sigma_i(t) = E_{\underline{i}}\left(\varepsilon_{\underline{i}}(t) - \beta^0_{\underline{i}}(t)\right)$$

$$\sigma_i(t) = \sigma_i^L(t) + E_{\underline{i}}\left[\sum_{\tau<t} D^{\varepsilon}_{\underline{i}k}(t+1-\tau)\beta^0_k(\tau) + \left(D^{\varepsilon}_{\underline{i}k}(1) - \delta_{\underline{i}k}\right)\beta^0_k(t)\right] \quad (6)$$

Let us assume that the *virtual distortions* simulate piece-wise linear constitutive relations of elasto-plastic material Fig. 1. These constitutive relations can be expressed as follows:

$$(1-\gamma_{\underline{i}})\left(\sigma_{\underline{i}}(t) - \mathrm{sign}\left(\sigma_{\underline{i}}^{TR}\right)\sigma^\star_{\underline{i}}\right) = \gamma_{\underline{i}}E_{\underline{i}}\left(\mathrm{sign}\left(\sigma_{\underline{i}}^{TR}\right)\alpha_{\underline{i}} + \Delta\beta^0_{\underline{i}}(t)\right) \quad (7)$$

where $\sigma_i^\star = E_{\underline{i}}\varepsilon^\star_{\underline{i}}$ denotes the plastic limit and γ_i denotes the hardening parameter in element i. The vector σ_i^{TR}

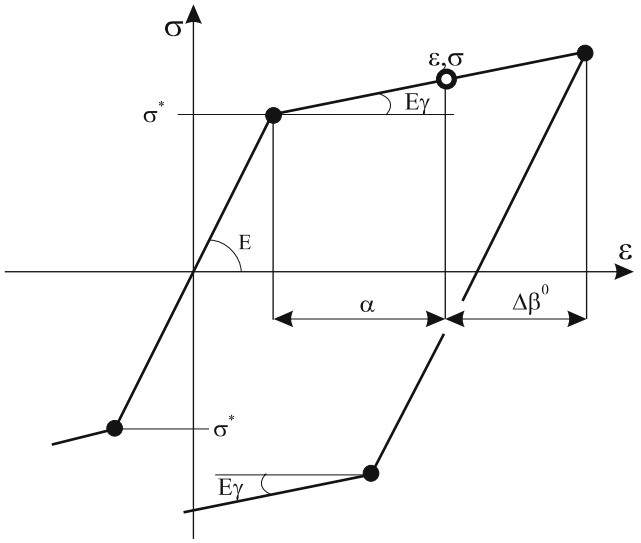

Fig. 1 Piece-wise linear elasto-plastic constitutive model

denotes the trial stress to be determined initially for each time step. These stresses can be calculated from (8) and are necessary for determination of the set of plastified elements and the sign of their stresses.

$$\sigma_i^{TR} = E_{\underline{i}} \left(\varepsilon_{\underline{i}}^{\neq t}(t) - \beta_{\underline{i}}^0(t-1) \right) \tag{8}$$

where $\varepsilon_i^{\neq t}(t)$ is a strain vector, in which the influence of plastic distortions $\beta_i^0(t)$ at the actual time step t was not taken into account.

The quantity α_i denotes the equivalent plastic strain for the isotropic hardening condition for element i and is defined as follows:

$$\alpha_i = \sum_t \left| \Delta\beta_i^0(t) \right| \tag{9}$$

where $\Delta\beta_i^0(t)$ denotes the increment of plastic distortion for the time step t.

It is convenient for the VDM method to express strains and stresses in such a way that increments of plastic distortions are explicitly shown for each time step. To this end, formula (5) can be rearranged as follows:

$$\varepsilon_i(t) = \varepsilon_i(t-1) + \Delta\varepsilon_i(t) \tag{10}$$

where the strain increment $\Delta\varepsilon_i(t)$ takes the form:

$$\Delta\varepsilon_i(t) = \Delta\varepsilon_i^L(t) + \sum_{\tau=1}^{t-1} D_{ik}^{\varepsilon}(t+1-\tau)\Delta\beta_k^0(\tau) + D_{ik}^{\varepsilon}(1)\Delta\beta_k^0(t) \tag{11}$$

Introducing additional components $\Delta\varepsilon_i^{\neq t}(t)$ describing strain increments without the actual increment of plastic distortions in the time step t, formula (10) can be expressed as follows:

$$\varepsilon_i(t) = \varepsilon_i(t-1) + \Delta\varepsilon_i^{\neq t}(t) + D_{ik}^{\varepsilon}(1)\Delta\beta_k^0(t) \tag{12}$$

Formula (6) describing the stresses can be also rearranged in such a way, that the increment of plastic distortions can be easily calculated:

$$\sigma_i(t) = \sigma_i(t-1) + E_{\underline{i}}\Delta\varepsilon_{\underline{i}}(t) - E_{\underline{i}}\Delta\beta_{\underline{i}}^0 \tag{13}$$

Substituting strains from (12) to the above formula, the final equation determining stresses can be received:

$$\sigma_i(t) = \sigma_i(t-1) + E_{\underline{i}}\Delta\varepsilon_{\underline{i}}^{\neq t}(t) + E_{\underline{i}}\left(D_{\underline{i}k}^{\varepsilon}(1) - \delta_{\underline{i}k} \right)\Delta\beta_k^0(t) \tag{14}$$

Taking into account the above relations, the increment of plastic distortions $\Delta\beta_k^0$ can be determined from the following set of equations:

$$\begin{aligned} &\left[E_{\underline{i}}\delta_{\underline{i}k} - (1-\gamma_{\underline{i}})E_{\underline{i}}D_{\underline{i}k}^{\varepsilon}(1) \right]\Delta\beta_k^0(t) \\ &\quad = (1-\gamma_{\underline{i}})\left(\sigma_{\underline{i}}(t-1) + E_{\underline{i}}\Delta\varepsilon_{\underline{i}}^{\neq t}(t) \right) \\ &\qquad - \operatorname{sign}\left(\sigma_i^{TR}\right)\left((1-\gamma_{\underline{i}})\sigma_i^{\star} + \gamma_{\underline{i}}E_{\underline{i}}\alpha_{\underline{i}} \right) \end{aligned} \tag{15}$$

Making use of the relation:

$$\sigma_i(t-1) + E_{\underline{i}}\Delta\varepsilon_{\underline{i}}^{\neq t}(t) = \sigma_i^{TR} \tag{16}$$

the set of equations (15) can be expressed in the final form:

$$\begin{aligned} &\left[E_{\underline{i}}\delta_{\underline{i}k} - (1-\gamma_{\underline{i}})E_{\underline{i}}D_{\underline{i}k}^{\varepsilon}(1) \right]\Delta\beta_k^0(t) \\ &\quad = (1-\gamma_{\underline{i}})\sigma_{\underline{i}}^{TR} - \operatorname{sign}\left(\sigma_{\underline{i}}^{TR}\right)\left((1-\gamma_{\underline{i}})\sigma_{\underline{i}}^{\star} + \gamma_{\underline{i}}E_{\underline{i}}\alpha_{\underline{i}} \right) \end{aligned} \tag{17}$$

A similar relation for the increment of plastic distortions $\Delta\beta^0(t)$ has been formulated in Simo and Huges (1998) via the so-called *return-mapping algorithm for rate-independent plasticity with isotropic hardening*.

Note that the principal matrix in the set of equations (17) is time-independent and has to be recalculated only when one or more elements enter the plastic zone.

The algorithm for elasto-plastic analysis is shown in Table 1.

3.1 Numerical testing

The dynamic response of an elasto-plastic structure (Fig. 2) has been calculated using the VDM method and

Table 1 Algorithm of IVDM-based modelling of physical nonlinearities

Data and initial calculations:

Input data
- Construction under external load
- Yield stress limits $\sigma^\star$, hardening parameter γ

Calculations
- Linear structural response ε^L
- Dynamic influence matrix $\mathbf{D}^\varepsilon(\mathbf{t})$
- Calculation of principal time independent matrix **F** for plasticity modelling (17)

Calculation for each time step t:

1. Strains $\varepsilon^{\neq \mathbf{t}}(\mathbf{t})$
   $\varepsilon_i^{\neq t}(t) = \varepsilon_i^L(t) + \sum_{\tau<t} D_{ik}^\varepsilon(t+1-\tau)\beta_i^0(\tau)$
2. Trial Stress
   $\sigma_i^{TR} = E_{\underline{i}}\left(\varepsilon_{\underline{i}}^{\neq t}(t) - \beta_{\underline{i}}^0(t-1)\right)$
3. Determination of plastic zone $\mathfrak{B}$
   $|\sigma_i^{TR}| > \sigma_i^\star + \frac{\gamma_{\underline{i}} E_{\underline{i}} \alpha_{\underline{i}}}{1-\gamma_{\underline{i}}}$
   YES
   (a) Update principal matrix **F**
   (b) Calculate plastic distortion increment $\Delta\beta_k^0(t)$ (17)
   (c) Update of plastic distortion:
   $\beta_k^0(t) = \beta_k^0(t-1) + \Delta\beta_k^0(t)$
   (d) Update equivalent plastic strain for isotropic hardening:
   $\alpha_k = \alpha_k + |\Delta\beta_k^0(t)|$
   (e) Update strains
   $\varepsilon_i(t) = \varepsilon_i^{\neq t}(t) + D_{ik}^\varepsilon \beta_k^0(t)$
   (f) Update stress
   $\sigma_i(t) = E_i(\varepsilon_i(t) - \beta_i^0(t))$
   (g) Check the sign $\Delta\beta_k^0(t)\sigma_k(t)$ If negative, go back to a) and update the principal matrix **F**
   NO
   (a) Taking in to account $\beta_k^0(t) = \beta_k^0(t-1)$ update strains:
   $\varepsilon_i(t) = \varepsilon_i^{\neq t}(t) + D_{ik}^\varepsilon(1)\beta_k^0(t)$
   (b) Stress:
   $\sigma_i(t) = \sigma_i^{TR}$
   (c) If necessary calculate displacements, velocities and accelerations.
4. Go to 1)

via the commercially available ANSYS package (2D truss element *LINK1* with *bilinear isotropic hardening*). The plastic limit $\sigma^\star$ and the hardening parameter γ have been assumed to be equal for all elements: 50 MPa and 0.01, respectively. As external load, an initial velocity of $V = 5$ m/s has been applied to node 2 in vertical direction.

The responses of plastic distortions in all elements have been selected to verify the results (Fig. 3). The obtained discrepancies are very small. Another way to verify the obtained results is checking the discrepancies in energy balance (Fig. 4).

Considering the insignificant discrepancies of the results obtained, for the comparison, an additional parameter, which characterizes a relative difference between the results, was introduced based on the formula:

$$\Delta e_i(t) = \frac{e_i^R(t) - e_i^{VDM}(t)}{e_i^R(t)} \tag{18}$$

where e is the determined value (strain, displacement, plastic distortion, etc.). The upper scripts $()^R$ and $()^{VDM}$

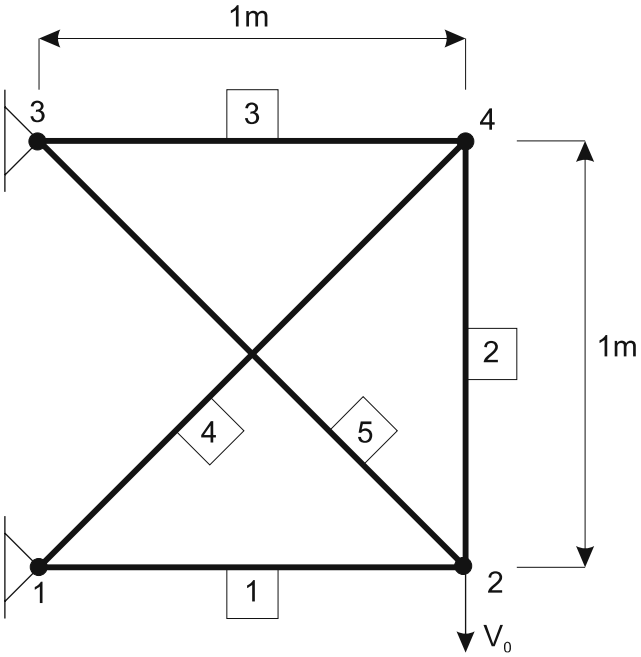

Fig. 2 The testing truss structure

denote the reference results and results from VDM, respectively. In the presented example, the reference values are plastic strains obtained via ANSYS.

The diagrams depicted in Fig. 5 present relative discrepancies (18) for plastic distortions $\boldsymbol{\beta}^0(t)$. The maximum value of relative discrepancies does not exceed 3.3% for the third element.

3.2 Sensitivity analysis for modification of plastic limit

Let us demonstrate the impulse virtual distortion method (IVDM)-based sensitivity analysis of elasto-plastic structures on the example of gradient calculation

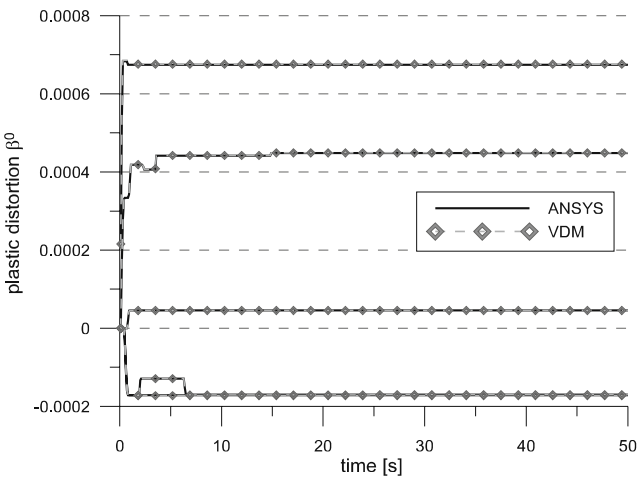

Fig. 3 Comparison of plastic distortions in all elements calculated via ANSYS and IVDM

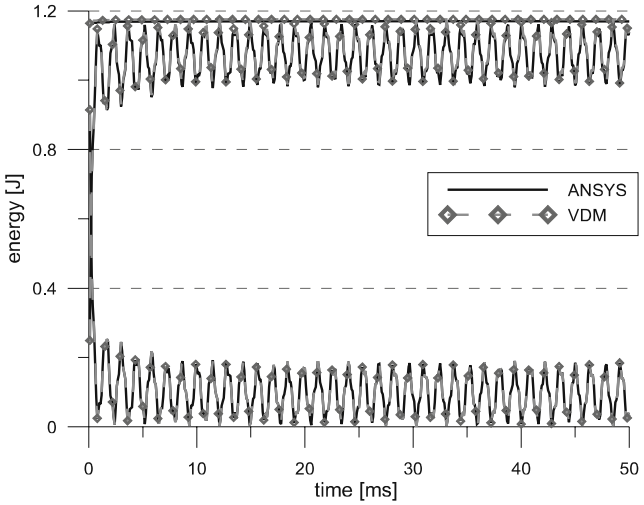

Fig. 4 Comparison of energy balance obtained via ANSYS and IVDM

for strains $\varepsilon(t)$, with respect to plastic limits $\sigma^{\star}$. To this end, the derivative of the strain formula has been determined:

$$\frac{\partial \varepsilon_i(t)}{\partial \sigma_l^{\star}} = \sum_{\tau \le t} \sum_{\tau' \le \tau} D_{ik}^{\varepsilon}(\tau + 1 - \tau') \frac{\partial \Delta \beta_k^0(\tau')}{\partial \sigma_l^{\star}} \tag{19}$$

The component $\frac{\partial \Delta \beta_k^0(t)}{\partial \sigma_l^{\star}}$ can be obtained differentiating formula (17):

$$\left[E_{\underline{i}}\delta_{\underline{i}k} - (1-\gamma_{\underline{i}})E_{\underline{i}}B_{\underline{i}k}^{\varepsilon}(1)\right]\frac{\partial \Delta \beta_k^0(t)}{\partial \sigma_l^{\star}} = \frac{\partial \sigma_{\underline{i}}^{TR}}{\partial \sigma_l^{\star}}(1-\gamma_{\underline{i}}) - \text{sign}\left(\sigma_{\underline{i}}^{TR}\right)\left((1-\gamma_{\underline{i}})\delta_{\underline{i}l} + \gamma_{\underline{i}}E_{\underline{i}}\frac{\partial \alpha_{\underline{i}}}{\partial \sigma_l^{\star}}\right) \tag{20}$$

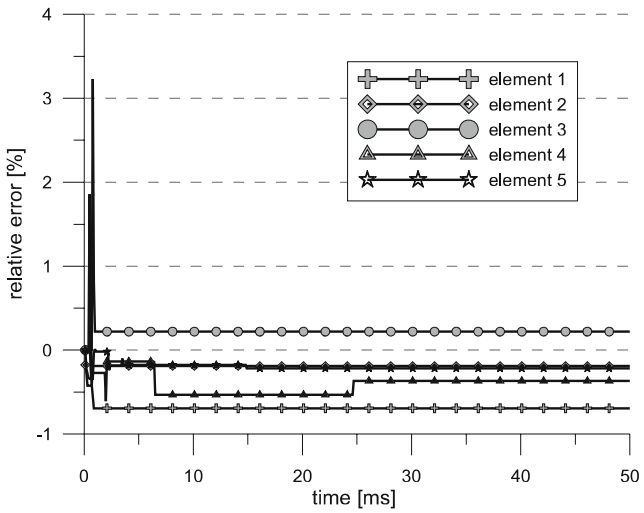

Fig. 5 The relative difference of plastic distortion

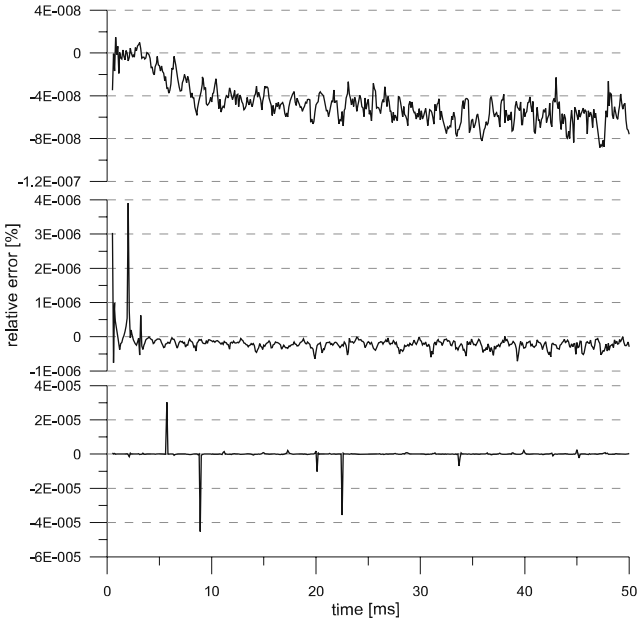

Fig. 6 The relative difference of strain field sensitivity for the first element with respect to yield stress limit for the first, second, and third elements

where $\frac{\partial \sigma_i^{TR}}{\partial \sigma_l^{\star}}$ is determined as follows:

$$\frac{\partial \sigma_{\underline{i}}^{TR}}{\partial \sigma_l^{\star}} = E_{\underline{i}}\left(\frac{\partial \varepsilon_{\underline{i}}^{\neq t}(t)}{\partial \sigma_l^{\star}} - \frac{\partial \beta_{\underline{i}}^0(t-1)}{\partial \sigma_l^{\star}}\right) \tag{21}$$

and $\frac{\partial \alpha_i}{\partial \sigma_l^{\star}}$ can be determined due to the following rules:

$$\frac{\partial \alpha_{\alpha}}{\partial \sigma_l^{\star}} = \sum_t \text{sign}\left(\Delta \beta_i^0(t)\right)\frac{\partial \Delta \beta_i^0(t)}{\partial \sigma_l^{\star}} \tag{22}$$

The diagrams depicted in Fig. 6 present the relative discrepancy value (18) for gradients (19) obtained via the finite differences method vs analytically determined gradients (VDM-based). The absolute discrepancy value was calculated for strains in the first element with respect to the yield stress limit in the first, second, and third elements (Fig. 6). The maximal values of discrepancies do not exceed $5e-5\%$.

4 Coupled problem of material redistribution with physical nonlinearities (modifications of: K, M, and $\sigma^{\star}$)

The simulation of material redistribution (modifications of element cross-sections A and associated stiffness and mass modifications) for a structure with elasto-plastic material characteristics will be presented in this section.

The equation of motion for elastic structural response of the initial structural configuration takes the form:

$$\mathbf{M}\ddot{\mathbf{u}}(t) + \mathbf{K}\mathbf{u}(t) = \mathbf{f}(t), \tag{23}$$

where matrices $\mathbf{M}$, $\mathbf{K}$ denote mass and stiffness matrices, respectively, and $\mathbf{f}(t)$ denotes external forces. Each matrix is composed of parameters that can be modified, causing modification of the above formula:

$$\big[\mathbf{M} + \Delta\mathbf{M}\big]\ddot{\mathbf{u}}(t) + \big[\mathbf{K} + \Delta\mathbf{K}\big]\mathbf{u}(t) = \mathbf{f}(t), \tag{24}$$

where $\Delta\mathbf{M}$ and $\Delta\mathbf{K}$ denote modifications of mass and stiffness matrix, respectively, taking into account physical nonlinearities. The equations of motion for the *modified* and *modelled* structures with virtual components simulating modifications of material distribution or physical nonlinearity (Wiklo and Holnicki-Szulc 2008) can be expressed as follows:

$$\hat{M}_{NM}\ddot{u}_M(t) + G^T_{Ni}\hat{S}_{ij}G_{jM}u_M(t) = f_N(t) \tag{25}$$

$$M_{NM}u_M(t) + G^T_{Ni}S_{ij}\Big[G_{jM}u_M(t) - l_{\underline{j}}\varepsilon^0_{\underline{j}}(t) - l_{\underline{j}}\beta^0_{\underline{j}}(t)\Big] = f_N(t) + p^0_N(t) \tag{26}$$

where $\hat{S}_{ij}$ and S_{ij} denote diagonal matrices with the following diagonal components: $\hat{S}_{ii} = E_{\underline{i}}\hat{A}_{\underline{i}}/l_{\underline{i}}$ and $S_{ii} = E_{\underline{i}}A_{\underline{i}}/l_{\underline{i}}$, respectively, E_i, the Young modulus; l_i, the length of element; A_i, the initial element cross-section; and $\hat{A}_i$, the modified element cross-section. Equation (26) can be also expressed via strains rather than displacements:

$$M_{NM}\ddot{u}_M(t) + G^T_{Ni}S_{ij}\Big[l_{\underline{j}}\Big(\varepsilon_{\underline{j}}(t) - \varepsilon^0_{\underline{j}}(t) - \beta^0_{\underline{j}}(t)\Big)\Big] = f_N(t) + p^0_N(t) \tag{27}$$

where the strain vector $\varepsilon_j(t)$ is defined through formula (3).

The dynamic structural response can be expressed as superposition of linear response and terms due to modifications simulated via virtual components:

$$u_N(t) = u^L_N(t) + \sum_{\tau\le t} B^{\varepsilon}_{Nj}(t+1-\tau)\varepsilon^0_j(\tau) + \sum_{\tau\le t} B^{\varepsilon}_{Nk}(t+1-\tau)\beta^0_k(\tau) + \sum_{\tau\le t} B^{p}_{NM}(t+1-\tau)p^0_M(\tau) \tag{28}$$

where vectors of virtual components $\varepsilon^0_j(t)$, $\beta^0_k(t)$, and $p^0_M(t)$ simulate modifications of element stiffness (virtual distortion), physical nonlinearity (plastic distortion), and element mass (virtual force), respectively. Indices N denote all degrees of freedom, indices j denote elements with cross-sections modified, k denote plastified elements, and M denotes degrees of freedom related to elements with cross-sections modified.

The updated strain $\varepsilon_i(t)$ can be obtained by multiplying formula (28) with the quantity $\frac{1}{L_{\underline{i}}}G_{\underline{i}M}$,

$$\varepsilon_i(t) = \varepsilon^L_i(t) + \sum_{\tau\le t} D^{\varepsilon}_{ij}(t+1-\tau)\varepsilon^0_j(\tau) + \sum_{\tau\le t} D^{\varepsilon}_{ik}(t+1-\tau)\beta^0_k(\tau) + \sum_{\tau\le t} D^{p}_{iM}(t+1-\tau)p^0_M(\tau) \tag{29}$$

were the matrices D^{ε}_{ij} and D^{p}_{iM} (defined in Wiklo and Holnicki-Szulc (2008)) were used to achieve equation (29). The strain (29) should be also rearranged separating the increment of plastic distortions:

$$\varepsilon_i(t) = \varepsilon^L_i(t) + \sum_{\tau\le t} D^{\varepsilon}_{ij}(t+1-\tau)\varepsilon^0_j(\tau) + \sum_{\tau\le t}\sum_{\hat{\tau}\le\tau} D^{\varepsilon}_{ik}(t+1-\hat{\tau})\Delta\beta^0_k(\hat{\tau}) + \sum_{\tau\le t} D^{p}_{iM}(t+1-\tau)p^0_M(\tau) \tag{30}$$

Defining the additional quantity $\varepsilon^{\neq t}_i(t)$ describing strains without effect of virtual components from the time step t, the expression for strains in the time step t can be modified as follows:

$$\varepsilon_i(t) = \varepsilon^{\neq t}_i(t) + D^{\varepsilon}_{ij}(1)\varepsilon^0_j(t) + D^{\varepsilon}_{ik}(1)\Delta\beta^0_k(t) + D^{p}_{iM}(1)p^0_M(t) \tag{31}$$

The main postulate of the IVDM method is that forces and strains of the *modified* and *modelled* structures are identical. The formula of this postulate will lead us to equations allowing the determination of virtual components simulating given structural modifications. To this end, the axial forces in elements of *modified* and *modelled* structures can be expressed as follows:

$$\hat{p}_i(t) = E_{\underline{i}}\hat{A}_{\underline{i}}\big(\varepsilon_{\underline{i}}(t) - \beta^0_{\underline{i}}(t)\big) \tag{32}$$

$$p_i(t) = E_{\underline{i}}A_{\underline{i}}\big(\varepsilon_{\underline{i}}(t) - \varepsilon^0_{\underline{i}}(t) - \beta^0_{\underline{i}}(t)\big) \tag{33}$$

Making use of these expressions, the modification parameters of the cross-section can be expressed as follows:

$$\mu_i^A \stackrel{\text{def}}{=} \frac{\hat{A}_{\underline{i}}}{A_{\underline{i}}} = \frac{\varepsilon_{\underline{i}}(t) - \beta_{\underline{i}}^0(t) - \varepsilon_{\underline{i}}^0(t)}{\varepsilon_{\underline{i}}(t) - \beta_{\underline{i}}^0(t)} \tag{34}$$

The modification parameters describe the proportion between the modified cross-section $\hat{A}_i$ and the original cross-section $A_{\,i}$. The parameters μ_i^A belong to the interval $\mu_i^A \in \langle 0, \mu_i^{\mathrm{A\,max}} \rangle$. $\mu_i^{\mathrm{A}} = 0$ means that the structural element i is eliminated; $\mu_i^{\mathrm{A}} = 1$ means that no modification is made, while $\mu_i^{\mathrm{A}} = \mu^{\mathrm{A\,max}}$ means that the maximal modification has been done.

Formula (34) can be rearranged in the following way:

$$\varepsilon_i^0(t) = \left(1 - \mu_{\underline{i}}^A\right)\left(\varepsilon_{\underline{i}}(t) - \beta_{\underline{i}}^0(t)\right) \tag{35}$$

and additionally, the increment of plastic distortion $\Delta\beta_i^0(t)$ can be shown explicitly to facilitate the computational algorithm:

$$\varepsilon_i^0(t) = \left(1 - \mu_{\underline{i}}^A\right)\left(\varepsilon_{\underline{i}}(t) - \beta_{\underline{i}}^0(t-1) - \Delta\beta_{\underline{i}}^0(t)\right) \tag{36}$$

Substituting formula (31) to (36), the first out of the three conditions necessary to determine the virtual components describing the coupled problem can be derived:

$$\begin{aligned}&\left[\delta_{ij} - \left(1 - \mu_{\underline{i}}^{\mathrm{A}}\right) D_{\underline{i}j}^{\varepsilon}(1)\right]\varepsilon_j^0(t) - \left(1 - \mu_{\underline{i}}^{\mathrm{A}}\right) D_{\underline{i}M}^{P}(1) p_M^0(t)\\ &\quad - \left(1 - \mu_{\underline{i}}^{\mathrm{A}}\right)\left[D_{\underline{i}k}^{\varepsilon}(1) - \delta_{\underline{i}k}\right]\Delta\beta_k^0(t)\\ &\quad = \left(1 - \mu_{\underline{i}}^{\mathrm{A}}\right)\left(\varepsilon_{\underline{i}}^{\neq t}(t) - \beta_{\underline{i}}^0(t-1)\right)\end{aligned} \tag{37}$$

The identity of inertia forces for the *modified* and *modelled* structure will give us the second necessary condition:

$$\hat{M}_{NM}\ddot{u}_M(t) = M_{NM}\ddot{u}_M(t) - p_N^0(t) \tag{38}$$

leading to the following form:

$$p_N^0(t) = -\Delta M_{NM}\ddot{u}_M(t) \tag{39}$$

where the mass matrix increment ΔM_{NM} is calculated via the formula (40), while the accelerations $\ddot{u}_M(t)$ can be determined from relation (41).

$$\Delta M_{NM} = \sum_i \left(\mu_{\underline{i}}^{\mathrm{A}} - 1\right) A_{\underline{i}}\rho_{\underline{i}} l_{\underline{i}} \overset{i}{a}{}_{Nr}^{T} M_{rs}^{el} \overset{i}{a}{}_{sM} \tag{40}$$

$$\begin{aligned}\ddot{u}_N(t) = \ddot{u}_N^L(t) &+ \sum_{\tau \le t} \ddot{B}_{Nj}^{\varepsilon}(t-\tau)\varepsilon_j^0(\tau)\\ &+ \sum_{\tau \le t} \ddot{B}_{NM}^{p}(t+1-\tau)p_M^0(\tau)\\ &+ \sum_{\tau \le t}\sum_{\hat{\tau} \le \tau} \ddot{B}_{Nk}^{\varepsilon}(t+1-\hat{\tau})\Delta\beta_K^0(\hat{\tau})\end{aligned} \tag{41}$$

Substituting (41) to (39), the second condition can be derived:

$$\begin{aligned}&\Delta M_{NM}\ddot{B}_{Mj}^{\varepsilon}(1)\varepsilon_j^0(t) + \left[\delta_{NM} + \Delta M_{NL}\ddot{B}_{LM}^{p}(1)\right]p_M^0(t)\\ &\quad + \Delta M_{NM}\ddot{B}_{Mk}^{\varepsilon}(1)\Delta\beta_k^0(t) = -\Delta M_{NM}\ddot{u}_M^{\neq t}(t)\end{aligned} \tag{42}$$

where $\ddot{u}_M^{\neq t}(t)$ describe accelerations without contribution of virtual components from the time step t.

The third condition necessary for the determination of the virtual components should be based on the formula modelling the modification of the constitutive relation, making distinction between two cases:

- For modification of the Young's modulus, the stresses can be described in the form:

$$\sigma_i(t) = E_{\underline{i}}\left(\varepsilon_{\underline{i}}(t) - \varepsilon_{\underline{i}}^0(t) - \beta_{\underline{i}}^0(t)\right) \tag{43}$$

- For modification of the cross-section A, the stresses (43) have to be scaled with the modification parameter (34):

$$\hat{\sigma}_i(t) = \frac{\sigma_{\underline{i}}(t)}{\mu_{\underline{i}}^A} = E_{\underline{i}}\left(\varepsilon_{\underline{i}}(t) - \beta_{\underline{i}}^0(t)\right) \tag{44}$$

4.1 Modification of the cross-section A in the coupled problem

Let us consider modifications of material distribution (modification of the cross-sections A) for the structure with elasto-plastic properties. In the constitutive relation, stresses scaled with the modification parameter $\boldsymbol{\mu}^{\mathrm{A}}$ (34) should be used in this case. To this end, the stresses (6) can be expressed in the form:

$$\begin{aligned}\sigma_i(t) = E_{\underline{i}}\Big(&\varepsilon_{\underline{i}}^{\neq t}(t) + D_{\underline{i}j}^{\varepsilon}(1)\varepsilon_j^0(t) + D_{\underline{i}M}^{p}(1)p_M^0(t)\\ &+ D_{\underline{i}k}^{\varepsilon}(1)\Delta\beta_k^0(t) - \Delta\beta_{\underline{i}}^0(t) - \beta_{\underline{i}}^0(t-1)\Big)\end{aligned} \tag{45}$$

Substituting stresses (45) and strains (31) to the constitutive relation (7), the following formula can be derived:

$$\begin{aligned}&\left[E_{\underline{i}}(1+\gamma_{\underline{i}})\delta_{ik}-E_{\underline{i}}B^{\varepsilon}_{\underline{i}k}(1)\right]\Delta\beta^0_k(t)-E_{\underline{i}}B^{\varepsilon}_{\underline{i}j}(1)\varepsilon^0_j(t)\\&\quad-E_{\underline{i}}B^{p}_{\underline{i}M}(1)p^0_M(t)\\&\quad=E_{\underline{i}}(\varepsilon^{\neq t}_{\underline{i}}(t)-\beta^0_{\underline{i}}(t-1))-\mathrm{sign}(\sigma^{TR}_i)\left(\sigma^{\star}_i+\gamma_{\underline{i}}E_{\underline{i}}\alpha_{\underline{i}}\right)\end{aligned}\tag{46}$$

Finally, the three formulas allowing the determination of virtual components simulating determined material redistribution take the form:

$$\mathbf{F}^S\mathbf{d}^0=\mathbf{b}\tag{47}$$

where:

$$\mathbf{F}^s=\begin{bmatrix}\left[\delta_{ij}-\left(1-\mu^{\mathrm{A}}_{\underline{i}}\right)D^{\varepsilon}_{\underline{i}j}(1)\right] & -\left(1-\mu^{\mathrm{A}}_{\underline{i}}\right)D^{p}_{\underline{i}M}(1) & -\left(1-\mu^{\mathrm{A}}_{\underline{i}}\right)\left[D^{\varepsilon}_{\underline{i}k}(1)-\delta_{\underline{i}k}\right]\\ \Delta M_{NM}\ddot{B}^{\varepsilon}_{Mj}(1) & \left[\delta_{NM}+\Delta M_{NL}\ddot{B}^{p}_{LM}(1)\right] & \Delta M_{NM}\ddot{B}^{\varepsilon}_{Mk}(1)\\ -E_{\underline{i}}B^{\varepsilon}_{\underline{i}j}(1) & -E_{\underline{i}}B^{p}_{\underline{i}M}(1) & \left[E_{\underline{i}}(1+\gamma_{\underline{i}})\delta_{ik}-E_{\underline{i}}B^{\varepsilon}_{\underline{i}k}(1)\right]\end{bmatrix}\tag{48}$$

$$\mathbf{d}^0=\begin{bmatrix}\varepsilon^0_j(t)\\ p^0_M(t)\\ \Delta\beta^0_k(t)\end{bmatrix}\tag{49}$$

$$\mathbf{b}=\begin{bmatrix}\left(1-\mu^{A}_{\underline{i}}\right)\left(\varepsilon^{\neq t}_{\underline{i}}(t)-\beta^0_{\underline{i}}(t-1)\right)\\ -\Delta M_{NM}\ddot{u}^{\neq t}_M(t)\\ \sigma^{TR}_i-\mathrm{sign}\left(\sigma^{TR}_i\right)\left(\sigma^{\star}_i+\gamma_{\underline{i}}E_{\underline{i}}\alpha_{\underline{i}}\right)\end{bmatrix}\tag{50}$$

The formula for the trial stress calculation (8) was used to achieve the above relations.

In the considered case material, redistribution also affects the plastic zone distribution. Therefore, a procedure for the plastic zone update after each time step (and modification of plastified or unloaded elements) is necessary. The algorithm for simulation of material redistribution for the coupled problem is shown in Table 2

Table 2 Algorithm for the simulation of cross-section redistribution for the coupled problem

`Data and initial calculations:`

Input data
- Construction under external load
- Localization of virtual components
- Yield stress limits $\sigma^{\star}$, hardening parameter γ, modification parameters μ

Calculations
- Linear structural response $\ddot{u}^L(t)$, $\varepsilon^L(t)$
- Dynamic influence matrix $\mathbf{B}(t)$, $\mathbf{D}(t)$, $\ddot{\mathbf{B}}(t)$
- Calculation of principal time independent matrix $\mathbf{F}$ for coupled problem (48)

`Calculation for each time step t:`

1. Strains $\varepsilon^{\neq t}(t)$ and accelerations $\ddot{u}^{\neq t}$
2. Trial Stress $\sigma^{TR}_i=E_{\underline{i}}\left(\varepsilon^{\neq t}_{\underline{i}}(t)-\beta^0_{\underline{i}}(t-1)\right)$
3. Determination of plastic zone $\mathfrak{B}$ $|\sigma^{TR}_i|>\sigma^{\star}_i+\frac{\gamma_{\underline{i}}E_{\underline{i}}\alpha_{\underline{i}}}{1-\gamma_{\underline{i}}}$

YES
- (a) Update principal matrix $\mathbf{F}$ (48)
- (b) Calculate virtual parameters: plastic distortion increment $\Delta\beta^0_k(t)$, virtual distortion $\varepsilon^0_j(t)$ and virtual forces $p^0_M(t)$ (47)
- (c) Update of plastic distortion: $\beta^0_k(t)=\beta^0_k(t-1)+\Delta\beta^0_k(t)$
- (d) Update equivalent plastic strain for isotropic hardening: $\alpha_k=\alpha_k+|\Delta\beta^0_k(t)|$
- (e) Update strains and accelerations according to calculated virtual parameters (31)
- (f) Update stress (44)
- (g) Check the sign $\Delta\beta^0_k(t)\sigma_k(t)$ If negative, go back to a) and update the principal matrix $\mathbf{F}$

NO
- (a) Update the principal matrix $\mathbf{F}$
- (b) Calculate virtual parameters: virtual distortions $\varepsilon^0_j(t)$ and virtual forces $p^0_M(t)$
- (c) Update strains, accelerations and stresses (according to calculated virtual parameters taking into account: $\beta^0_k(t)=\beta^0_k(t-1)$
- (d) If necessary calculate displacements and velocities

4. If necessary calculate the sensitivity components
5. Go to 1)

4.2 Numerical test

Testing example Fig. 2 has been used to verify the results obtained via the virtual component methods (IVDM + impulse virtual force method) vs the reanalysis performed with the commercially available package ANSYS (2D truss element LINK1 and *bilinear isotropic hardening*).

Uniformly distributed plastic limits $\sigma^{\star}=50MPa$ and the hardening coefficient $\gamma=0.01$ have been assumed. The modification parameters μ^{A} shown in Table. 3 have been selected, while dynamic excitation is caused by an initial velocity $V=20$ m/s applied to node 2 in vertical direction.

The results are demonstrated below, where Fig. 7 shows the plastic distortions calculated via the VDM-based methods vs ANSYS results (Fig. 8). Figure 9 demonstrates virtual distortions simulating stiffness modifications, and Fig. 10 shows virtual forces simulating modifications of the mass distribution calculated via the VDM-based methods. Finally, Fig. 11

Table 3 Modifications of cross-sections to the five-element truss structure

Elem. No.	$\sigma^{\star}[Pa]$	γ	A	μ^{A}	$\hat{A}$
1	5.0×10^7	0.01	1×10^{-5}	0.8	8×10^{-6}
2	5.0×10^7	0.01	1×10^{-5}	1.1	1.1×10^{-5}
3	5.0×10^7	0.01	1×10^{-5}	0.6	6×10^{-6}
4	5.0×10^7	0.01	1×10^{-5}	0.2	2×10^{-6}
5	5.0×10^7	0.01	1×10^{-5}	0.7	7×10^{-6}

shows the energy balance calculated via the VDM-based methods vs ANSYS results. The maximal observed relative discrepancies (Fig. 8) are below 2%.

4.3 Modifications of mass and stiffness in the coupled problem

If structural remodelling is caused by material modifications (its density and stiffness) rather than by modification of element cross-sections, formula (43) for determining stresses should be applied to the constitutive relation. In consequence, the first out of the three necessary conditions (cf. (47) from the previous part) allowing determination of the virtual components takes the following, modified form:

$$\begin{aligned}&\left[E_{\underline{i}}\delta_{\underline{i}k}-(1-\gamma_{\underline{i}})E_{\underline{i}}B^{\varepsilon}_{\underline{i}k}(1)\right]\Delta\beta^0_k(t)-E_{\underline{i}}\left(B^{\varepsilon}_{\underline{i}j}(1)-\delta_{\underline{i}j}\right)\varepsilon^0_j(t)\\&\quad-E_{\underline{i}}B^{p}_{\underline{i}M}(1)\,p^0_M(t)\\&\quad=(1-\gamma_{\underline{i}})E_{\underline{i}}\left(\varepsilon^{\neq t}_{\underline{i}}(t)-\beta^0_{\underline{i}}(t-1)\right)\\&\qquad-\operatorname{sign}\left(\sigma_i^{TR}\right)\left((1-\gamma_{\underline{i}})\sigma^{\star}_{\underline{i}}+\gamma_{\underline{i}}E_{\underline{i}}\alpha_{\underline{i}}\right)\end{aligned}\tag{51}$$

The algorithm for the coupled problem with modification of material density and stiffness has to be updated as well (Table 4), taking into account that the development of the plastic zone should be estimated on the basis of trial stresses (16), which are to be determined at the initiation of each time loop and taking into account the virtual distortions $\varepsilon^0_i(t)$ simulating stiffness modifications:

$$\sigma_i^{TR}=E_{\underline{i}}\left(\varepsilon^{\neq t}_{\underline{i}}(t)-\varepsilon^0_{\underline{i}}(t)-\beta^0_{\underline{i}}(t-1)\right)\tag{52}$$

The decision about further development of the plastic zone can be made in two ways:

- Comparing the sign of stresses $\sigma(t)$ with the sign of plastic distortion increments $\Delta\beta^0(t)$, and modifying the set of plastified elements accordingly
- Initial evaluation of virtual distortions modelling stiffness modifications (treating the problem as decoupled) on the base of the following formula:

$$\varepsilon^0_i(t)=\left(1-\mu^{\mathrm{E}}_{\underline{i}}\right)\left(\varepsilon_{\underline{i}}(t)-\beta^0_{\underline{i}}(t)\right)\tag{53}$$

4.4 Numerical test

The testing example Fig. 2 from the previous part has been used to verify obtained results, assuming material

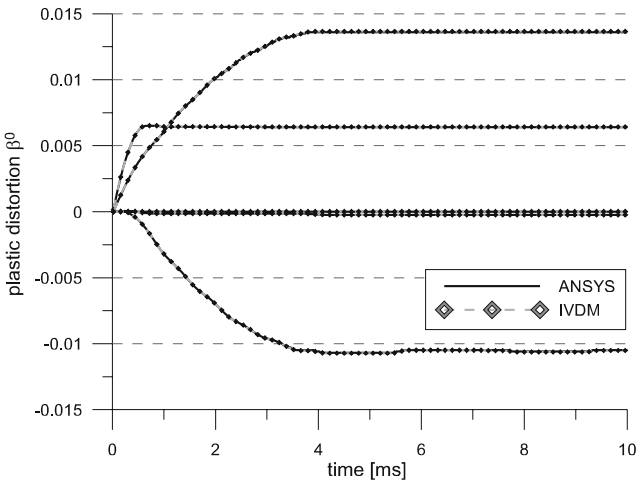

Fig. 7 Plastic distortions calculated via the VDM-based methods vs ANSYS results

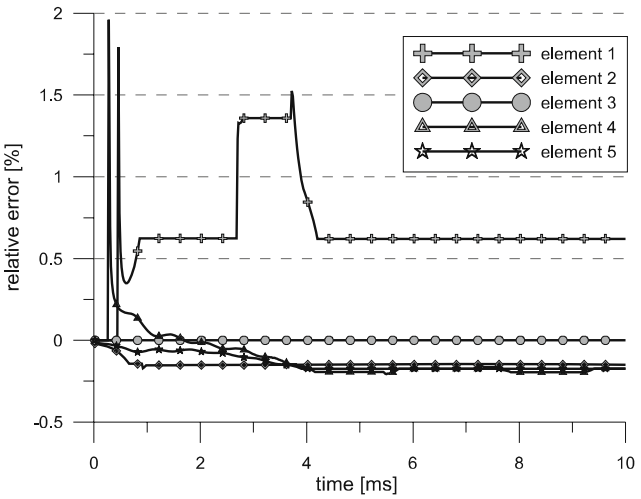

Fig. 8 Relative difference of plastic distortion

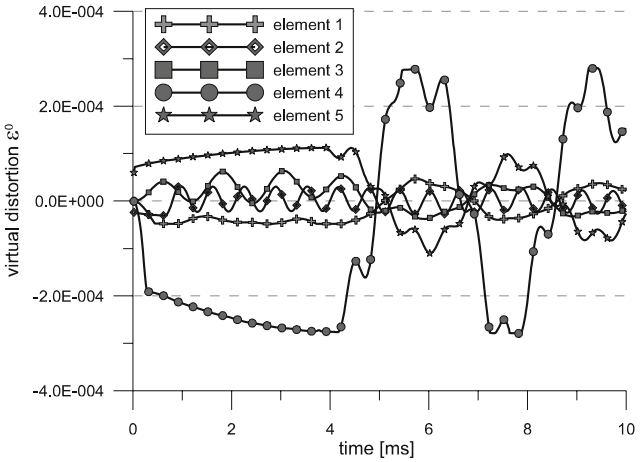

Fig. 9 Virtual distortions simulating stiffness modifications calculated via the VDM-based methods

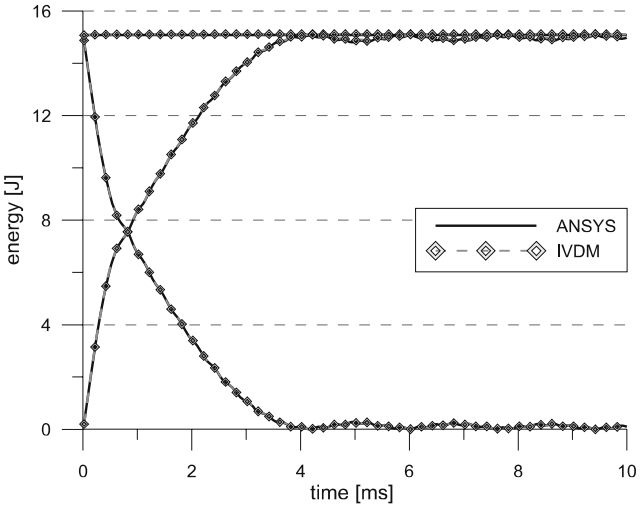

Fig. 11 Energy balance calculated via the VDM-based methods vs ANSYS results

modifications. The material in element 3 has been changed from steel to magnesium and those in elements 4 and 5 from steel to copper. The corresponding modifications of material densities and stiffness are shown in Table 5 (Kolakowski et al. 2007).

The above results (Figs. 12 and 13) demonstrate that discrepancies between the VDM-based and ANSYS approaches are very small and almost invisible.

4.5 Sensitivity analysis for the coupled problem

The advantage of the VDM based methods of structural remodelling is the analytical sensitivity analysis offering precise gradient computation. Let us demonstrate this possibility calculating the gradient of the objective function describing the increment of energy dissipation in the process of plastic yielding:

$$\Delta U(t) = \sigma_{\underline{i}}(t)\Delta\beta^0_{\underline{i}}(t) l_{\underline{i}} A_{\underline{i}} \mu_{\underline{i}} \tag{54}$$

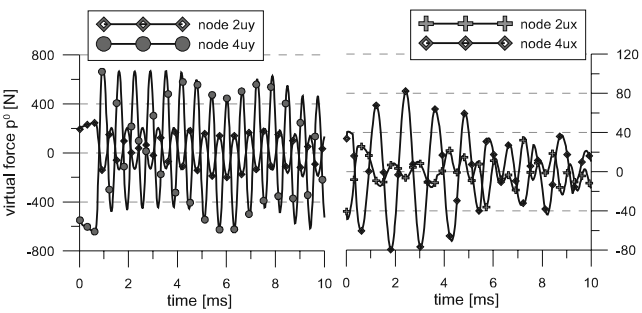

Fig. 10 Virtual forces simulating modifications of mass distribution calculated via the VDM-based methods

The derivative of this objective function with respect to the local cross-section modification can be expressed as follows:

$$\frac{\partial \Delta U(t)}{\partial \hat{A}_l} = \frac{\partial \sigma_{\underline{i}}(t)}{\partial \hat{A}_l}\Delta\beta^0_{\underline{i}}(t) A_{\underline{i}} l_{\underline{i}} \mu_{\underline{i}} + \frac{\partial \Delta\beta^0_{\underline{i}}(t)}{\partial \hat{A}_l}\sigma_{\underline{i}}(t) A_{\underline{i}} l_{\underline{i}} \mu_{\underline{i}} + \sigma_{\underline{i}}(t)\Delta\beta^0_{\underline{i}}(t) l_{\underline{i}} \delta_{il} \tag{55}$$

Where the component $\frac{\partial \sigma_{\underline{i}}(t)}{\partial \hat{A}_l}$ can be determined from the relation:

$$\frac{\partial \sigma_{\underline{i}}(t)}{\partial \hat{A}_l} = E_{\underline{i}}\left(\frac{\partial \varepsilon_{\underline{i}}(t)}{\partial \hat{A}_l} - \frac{\partial \beta^0_{\underline{i}}(t)}{\partial \hat{A}_l}\right) \tag{56}$$

The sensitivity of virtual components for the coupled problem has to be analyzed taking into account the set of three conditions (cf. (47)) determining these components simulating structural modifications. Now, our objective is to determine the related set of three conditions determining the gradient of the virtual components with respect to element cross-sections.

First, let us differentiate the formula (36) describing the virtual distortion $\varepsilon^0_i(t)$ with respect to the element cross-section:

$$\frac{\partial \varepsilon^0_i(t)}{\partial \hat{A}_l} = \left(1 - \mu^A_{\underline{i}}\right)\left(\frac{\partial \varepsilon_{\underline{i}}(t)}{\partial \hat{A}_l} - \frac{\partial \beta^0_{\underline{i}}(t)}{\partial \hat{A}_l}\right) - \frac{\partial \mu^{\mathrm{A}}_{\underline{i}}}{\partial \hat{A}_l}\left(\varepsilon_{\underline{i}}(t) - \beta^0_{\underline{i}}(t)\right) \tag{57}$$

After rearranging this equation and substituting the quantity $\frac{\partial \varepsilon^{\neq t}_{\underline{i}}(t)}{\partial \hat{A}_l}$, expressing the sensitivity with neglected

Table 4 Algorithm for simulation of material redistribution for the coupled problem

Data and initial calculations:

Input data
- Construction under external load
- Localization of virtual components
- Yield stress limits $\sigma^{\star}$, hardening parameter γ, modification parameters μ

Calculations
- Linear structural response $\ddot{u}^{L}(t)$, $\varepsilon^{L}(t)$
- Dynamic influence matrix $\mathbf{B}(t)$, $\mathbf{D}(t)$, $\ddot{\mathbf{B}}(t)$
- Calculation of principal time independent matrix **F** for coupled problem (48)

Calculation for each time step t:

1. Strains $\varepsilon^{\neq t}(t)$ and accelerations $\ddot{u}^{\neq t}$
2. Initial evaluation of virtual distortions $\varepsilon_i^0(t) = \left(1-\mu_{\underline{i}}^{\mathrm{E}}\right)\left(\varepsilon_{\underline{i}}(t) - \beta_{\underline{i}}^0(t)\right)$
3. Trial Stress $\sigma_i^{TR} = E_{\underline{i}}\left(\varepsilon_{\underline{i}}^{\neq t}(t) - \beta_{\underline{i}}^0(t-1)\right)$
4. Determination of plastic zone $\mathfrak{B}$ $|\sigma_i^{TR}| > (\sigma_i^{\star} + \gamma_{\underline{i}} E_{\underline{i}} \alpha_{\underline{i}})$

   YES
   (a) Update principal matrix **F** (48)
   (b) Calculate virtual parameters: plastic distortion increment $\Delta\beta_k^0(t)$, virtual distortion $\varepsilon_j^0(t)$ and virtual forces $p_M^0(t)$ (47)
   (c) Update of plastic distortion: $\beta_k^0(t) = \beta_k^0(t-1) + \Delta\beta_k^0(t)$
   (d) Update equivalent plastic strain for isotropic hardening: $\alpha_k = \alpha_k + |\Delta\beta_k^0(t)|$
   (e) Update strains and accelerations according to calculated virtual parameters (31)
   (f) Update stress (44)
   (g) Check the sign $\Delta\beta_k^0(t)\sigma_k(t)$ If negative, go back to a) and update the principal matrix **F**

   NO
   (a) Update the principal matrix **F**
   (b) Calculate virtual parameters: virtual distortions $\varepsilon_j^0(t)$ and virtual forces $p_M^0(t)$
   (c) Update strains, accelerations and stresses (according to calculated virtual parameters taking into account: $\beta_k^0(t) = \beta_k^0(t-1)$
   (d) If necessary calculate displacements and velocities
5. If necessary calculate the sensitivity components
6. Go to 1)

influence of the current time step t and described in the form:

$$\frac{\partial \varepsilon_i^{\neq t}(t)}{\partial \hat{A}_l} = \sum_{\tau=1}^{t-1} D_{ij}^{\varepsilon}(t-\tau)\frac{\partial \varepsilon_j^0(\tau)}{\partial \hat{A}_l} + \sum_{\tau=1}^{t-1} D_{iM}^{p}(t-\tau)\frac{\partial p_M^0(\tau)}{\partial \hat{A}_l} + \sum_{\tau=1}^{t}\sum_{\hat{\tau}=1}^{\tau-1} D_{ik}^{\varepsilon}(\tau-\hat{\tau})\frac{\partial \Delta\beta_k^0(\hat{\tau})}{\partial \hat{A}_l} \tag{58}$$

Table 5 Density and mass modifications

Element	μ^{E}	μ^{ρ}	$\sigma^{\star}$	γ
1	1.00	1.00	294	0.01
2	1.00	1.00	294	0.01
3	0.12	0.22	120	0.01
4	0.62	1.14	210	0.01
5	0.62	1.14	210	0.01

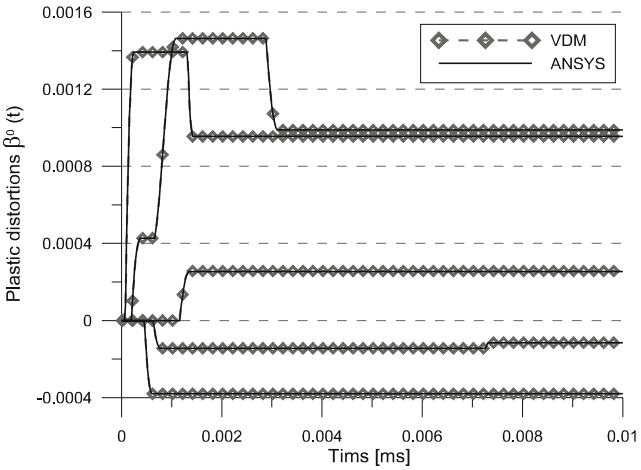

Fig. 12 Plastic distortions calculated via the VDM-based methods vs ANSYS results for material modifications

the first searched condition for the sensitivity analysis takes the form:

$$\left[\delta_{ij} - \left(1-\mu_{\underline{i}}^{\mathrm{A}}\right) D_{\underline{i}j}^{\varepsilon}(1)\right]\frac{\partial \varepsilon_j^0(t)}{\partial \hat{A}_l} - \left(1-\mu_{\underline{i}}^{\mathrm{A}}\right) D_{\underline{i}M}^{P}(1)\frac{\partial p_M^0(t)}{\partial \hat{A}_l} - \left(1-\mu_{\underline{i}}^{\mathrm{A}}\right) \times \left[D_{\underline{i}k}^{\varepsilon}(1) - \delta_{\underline{i}k}\right]\frac{\partial \Delta\beta_k^0(t)}{\partial \hat{A}_l} = \left(1-\mu_{\underline{i}}^{A}\right)\left(\frac{\partial \varepsilon_{\underline{i}}^{\neq t}(t)}{\partial \hat{A}_l} - \frac{\partial \beta_{\underline{i}}^0(t-1)}{\partial \hat{A}_l}\right) - \frac{\partial \mu_{\underline{i}}^{\mathrm{A}}}{\partial \hat{A}_l}\left(\varepsilon_{\underline{i}}(t) - \beta_{\underline{i}}^0(t)\right) \tag{59}$$

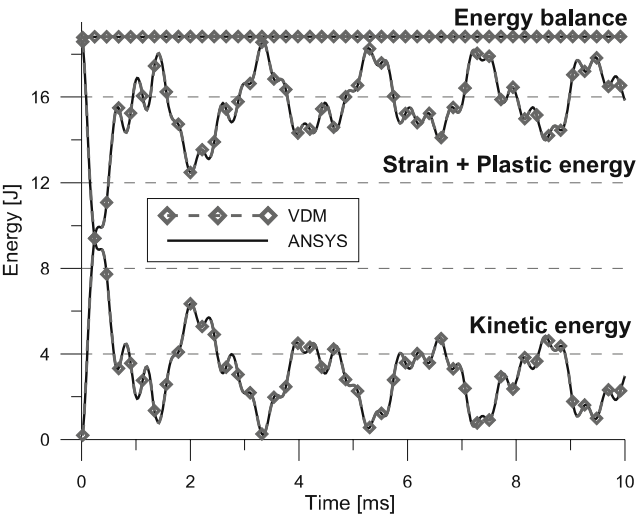

Fig. 13 Energy balance calculated via the VDM-based methods vs ANSYS results for material modifications

where

$$\frac{\partial \mu_i^{\mathrm{A}}}{\partial \hat{A}_l} = \frac{1}{\hat{A}_l}\delta_{il} \tag{60}$$

The second necessary condition for the sensitivity analysis can be obtained by differentiating (39):

$$\frac{\partial p_N^0(t)}{\partial \hat{A}_l} = -\frac{\partial \Delta M_{NM}}{\partial \hat{A}_l}\ddot{u}_M(t) - \Delta M_{NM}\frac{\partial \ddot{u}_M(t)}{\partial \hat{A}_l} \tag{61}$$

and rearranging the above formula:

$$\begin{aligned}
&\Delta M_{NM}\ddot{B}^{\varepsilon}_{Mj}(1)\frac{\partial \varepsilon_j^0(t)}{\partial \hat{A}_l} + \left[\delta_{NM} + \Delta M_{NL}\ddot{B}^{p}_{LM}(1)\right] \\
&\quad\times \frac{\partial p_M^0(t)}{\partial \hat{A}_l} + \Delta M_{NM}\ddot{B}^{\varepsilon}_{Nk}(1)\frac{\partial \Delta\beta_k^0(t)}{\partial \hat{A}_l} \\
&\quad= -\frac{\partial \Delta M_{NM}}{\partial \hat{A}_l}\ddot{u}_M(t) - \Delta M_{NM}\frac{\partial \ddot{u}_M^{\neq t}(t)}{\partial \hat{A}_l}
\end{aligned} \tag{62}$$

where $\frac{\partial \ddot{u}_M^{\neq t}(t)}{\partial \hat{A}_l}$ describes the sensitivity of the displacement field with respect to modification of the element cross-section $\hat{A}$, without sensitivity of virtual components in the current time step, and the component $\frac{\partial \Delta M_{NM}}{\partial \hat{A}_l}$ can be determined from the relation:

$$\frac{\partial \Delta M_{NM}}{\partial A_l} = \rho_{\underline{l}} l_{\underline{l}}\, \overset{i}{a}{}^{T}_{Nr} M^{el}_{rs}\, \overset{i}{a}{}_{sM} \tag{63}$$

The last necessary condition of the coupled sensitivity analysis can be obtained differentiating (46) with respect to the cross-sectional modification $\hat{A}$:

$$\begin{aligned}
&- E_{\underline{i}}B^{\varepsilon}_{\underline{i}j}(1)\frac{\partial \varepsilon_j^0(t)}{\partial \hat{A}_l} - E_{\underline{i}}B^{p}_{\underline{j}M}(1)\frac{\partial p_M^0(t)}{\partial \hat{A}_l} \\
&\quad + \left[E_{\underline{i}}(1+\gamma_{\underline{i}})\delta_{ik} - E_{\underline{i}}B^{\varepsilon}_{\underline{i}k}(1)\right]\frac{\partial \Delta\beta_k^0(\hat{\tau})}{\partial \hat{A}_l} \\
&\quad = E_{\underline{i}}\left(\frac{\partial \varepsilon_{\underline{i}}^{\neq t}(t)}{\partial \hat{A}_l} - \frac{\partial \beta_{\underline{i}}^0(t-1)}{\partial \hat{A}_l}\right) \\
&\qquad - \mathrm{sign}(\sigma_{\underline{i}}^{TR})\left(\gamma_{\underline{i}}E_{\underline{i}}\frac{\partial \alpha_{\underline{i}}}{\partial \hat{A}_l}\right)
\end{aligned} \tag{64}$$

where component $\frac{\partial \alpha_{\underline{i}}}{\partial \hat{A}_l}$ is described by the formula (22).

Finally, the equations of the coupled sensitivity analysis take the form:

$$\mathbf{F}^{\mathrm{S}}\mathbf{g}^0 = \mathbf{b}^{\mathrm{g}} \tag{65}$$

where the matrix $\mathbf{F}^S$ is identical to that from the coupled problem simulation (48) and vector $\mathbf{g}^0$ takes the form:

$$\mathbf{g^0} = \begin{bmatrix} \frac{\partial \varepsilon_j^0(t)}{\partial \hat{A}_l} \\ \frac{\partial p_M^0(t)}{\partial \hat{A}_l} \\ \frac{\partial \Delta\beta_k^0(t)}{\partial \hat{A}_l} \end{bmatrix}, \tag{66}$$

while the right-hand-side vector is given by:

$$\mathbf{b^g} = \begin{bmatrix} c\left(1-\mu_{\underline{i}}^{A}\right)\left(\frac{\partial \varepsilon_{\underline{i}}^{\neq t}(t)}{\partial \hat{A}_l} - \frac{\partial \beta_{\underline{i}}^0(t-1)}{\partial \hat{A}_l}\right) - \frac{\partial \mu_{\underline{i}}^{A}}{\partial \hat{A}_l}\left(\varepsilon_i(t) - \beta_{\underline{i}}^0(t-1)\right) \\ -\frac{\partial \Delta M_{NM}}{\partial \hat{A}_l}\ddot{u}_M(t) - \Delta M_{NM}\frac{\partial \ddot{u}_M^{\neq t}(t)}{\partial \hat{A}_l} \\ \frac{\partial \sigma_{\underline{i}}^{TR}}{\partial \hat{A}_l} - \mathrm{sign}(\sigma_i^{TR})\left(\gamma_{\underline{i}}E_{\underline{i}}\frac{\partial \alpha_{\underline{\alpha}}}{\partial \hat{A}_l}\right) \end{bmatrix} \tag{67}$$

The last component to be determined is the sensitivity of the strain field [cf. (58)] with respect to modification of the element cross-section. It can be done using formula (31):

$$\begin{aligned}
\frac{\partial \varepsilon_i(t)}{\partial \hat{A}_l} &= \frac{\partial \varepsilon_i^{\neq t}(t)}{\partial \hat{A}_l} + D^{p}_{iM}(1)\frac{\partial p_M^{0M}(t)}{\partial \hat{A}_l} + D^{\varepsilon}_{ij}(1)\frac{\partial \varepsilon_j^0(t)}{\partial \hat{A}_l} \\
&\quad + D^{\varepsilon}_{ik}(1)\frac{\partial \beta_k^0(t)}{\partial \hat{A}_l}
\end{aligned} \tag{68}$$

The sensitivity analysis has been performed for the testing example Fig. 2 with the data parameters defined in Table 5. As objective function, the global dissipation of energy through plastic yielding was applied:

$$U = \sum_t \Delta U(t) \tag{69}$$

The relative discrepancy values for gradients obtained via the finite differences method vs analytically determined gradients (using the VDM-based approach) are shown in Table 6. The discrepancy value does not exceed 5e-5.

Table 6 Comparison of the objective function sensitivity for the coupled problem

	MRS	IMDW	Discrepancy
$\frac{\partial U}{\partial \hat{A}_1}$	0.996206E+04	0.996205E+04	0.833870E-06
$\frac{\partial U}{\partial \hat{A}_2}$	0.204749E+05	0.204739E+05	0.467989E-04
$\frac{\partial U}{\partial \hat{A}_3}$	0.259559E+05	0.259552E+05	0.300264E-04
$\frac{\partial U}{\partial \hat{A}_4}$	0.443956E+06	0.443955E+06	0.250197E-05
$\frac{\partial U}{\partial \hat{A}_5}$	0.610193E+06	0.610192E+06	0.176812E-05

5 Optimal design of adaptive structures

Having developed the VDM-based technique for fast modifications (including simultaneous material redistributions and its nonlinearities) and sensitivity analysis for these modifications of structures exposed to dynamic loads, the optimal design problem for *adaptive structures* can be formulated. Assuming that properly located, actively controlled dissipaters (*structural fuses*) can perform similarly to elasto-plastic structural elements, the numerical tools presented above can be used for the optimal design of smart structures adapting in real time to random impact loads.

To this end, let us formulate the problem as follows:

1. Assume an initial structural configuration (made of a volume V of material) exposed to a set of determined, potential impact loads
2. Redesign the initial structural configuration in such a way that, by applying only a few controllable elements (as few as possible) with plastic-like response and the same material volume V, the response of adaptive structure to all possible impact loads will satisfy the compromise criterion imposed on average deflections and the impact absorption capacities

Now, let us postulate the following methodology via decomposition of this challenging problem into three stages:

1. Redesign the initial structural configuration (material redistribution causing topology modification) leading to *the stiffest structure* (average deflections minimized) under multi-impact load. The result of this remodelling is a new, close to isostatic structural topology with mass concentrated in a small number of elements and a significant reduction of maximal stresses induced in the impacted structure.
2. Determine optimal locations for *structural fuses*—elements with controllable elasto-plastic properties in the above-determined stiffest structure. It is crucial to find only few locations (controllable devices' cost minimization) allowing significant improvement of the structural response.
3. The *adaptive structure* is configured according to the No. 1 solution and equipped with active elements (locations determined in the No. 2 solution) and is exposed to randomly generated impacts from the predetermined set of potential loads. Assuming that this impact load can be identified in real time (Sekua et al. 2006), the optimal *adaptation* of the *adaptive structure* can be performed due to the requirement of maximal impact load dissipation.

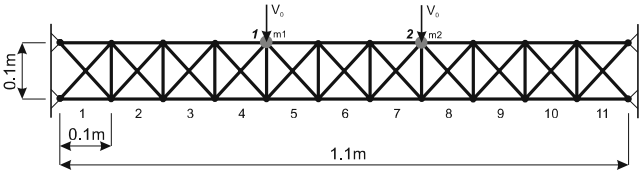

Fig. 14 The initial structural configuration

The above methodology of optimal remodelling of adaptive structures is illustrated below in the example of a truss-beam structure, where the overall effects of significant increase of impact load capacity and the impact energy dissipation are presented.

Let us continue the discussion of the truss structure example presented in the first part of this paper (Wiklo and Holnicki-Szulc 2008), Fig. 14, where the stiffest structure exposed to two potential impacts was determined (No. 1 solution). It is natural to apply two structural fuses located in the upper layer of two sections 1, 2 and 10, 11 (No. 2 solution, Fig. 15). Only two structural fuses located in elements accumulating the largest portion of strain energy in the elastic solution (No. 1 solution) are good candidates for location of the energy dissipation process. However, in the case of the one possible scenario of impact load (equation `m1 > m2` case), better locations for structural fuses are sections 10,11 (upper layer) and section 11 (lower layer).

Having determined the optimally remodelled structure equipped with structural fuses (Fig. 15), the problem of optimal adaptation to the identified real-time impact load (from the set of assumed, potential dynamic loads) leads to the determination of such time-invariant plastic stress limits $\sigma_i^\star$ in the controllable elements that the plastic-like energy dissipation (70) integrated in the assumed time interval $\langle 0, \tilde{t} \rangle$ is maximized:

$$\max = \sum_{\tilde{t}} \sum_{i} \sigma_i(t) \Delta\beta_i^0(t) l_i A_i \mu_i \tag{70}$$

where l_i, A_i, μ_i are the elements' length, cross-section, and modification parameter, respectively, and $\Delta\beta_i^0(t)$ and $\sigma_i(t)$ are the plastic distortion increment and stress

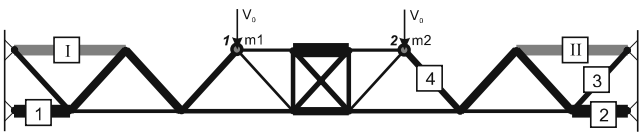

Fig. 15 Optimally remodelled structure with selected adaptive elements I and II

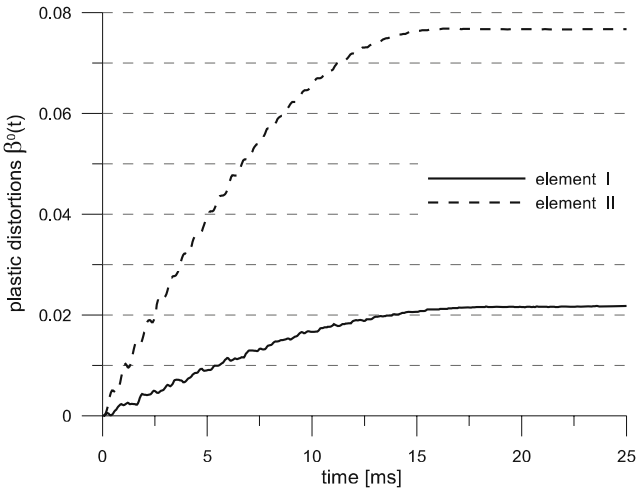

Fig. 16 Development of plastic distortions in adaptive elements No. I and II (adaptive structure Fig. 15)

in element i for the given time step t. The time integration interval should be defined determining $\tilde{t}$: $t_1 < \tilde{t} < t_2$, where t_1 denotes the instant of maximal load pick received by the elastic structure, while t_2 denotes the instant when the elastic spring back process starts. Too small values of $\tilde{t}$ can cause fast reaching of the constraints (72) and large residual vibrations after the impact process. Contrarily, too large values of $\tilde{t}$ can cause higher decelerations in the first phase of the impact process.

The maximization problem (70) is subject to the equations of motion, constitutive relations, and the following inequality constraints imposed on stress limits and total plastic-like distortions (stroke of the structural fuse dissipater):

$$|\sigma(t)| < \tilde{\sigma} \tag{71}$$

$$\left|\beta^0(t)\right| < \tilde{\beta} \tag{72}$$

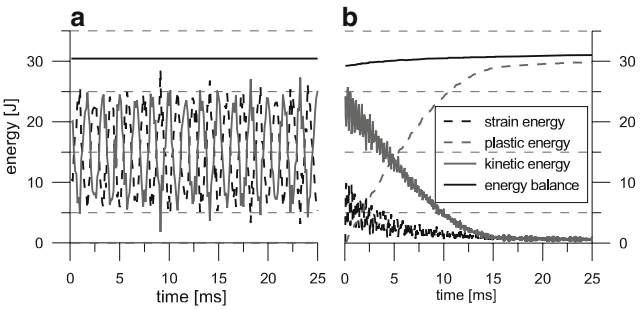

Fig. 17 Energy balance for **a** the initial structural configuration and **b** the optimal adaptive structure

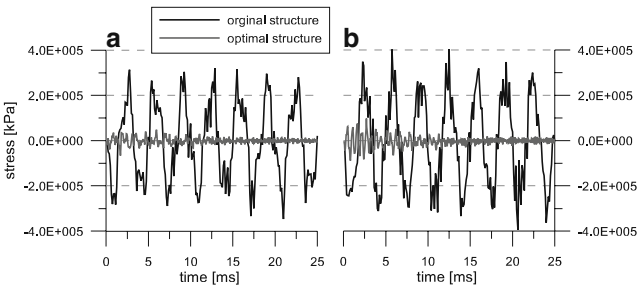

Fig. 18 Development of stresses in maximally loaded elements **a** No. 1, **b** No. 2. (adaptive structure Fig. 15)

The gradient-based optimization procedure (making use of the numerical tools described above) leads to the solution presented in the figures below. Figure 16 demonstrates the development of plastic distortions in the adaptive elements with the yield stresses fixed on the optimal levels: σ_I^*=2.8 MPa σ_{II}^*=3.6 MPa. The energy balance for the optimal adaptive structure and the initial one is shown in Fig. 17. Figures 18 and 19 present the stress development for the initial structural configuration vs the adaptive structure (significant reduction of stress levels in selected, maximally loaded elements No. 1, 2, 3, and 4, defined in Fig. 15). Comparison of the results presented below demonstrates the final effect of adaptive impact absorption by the optimally designed *adaptive structure* vs the elastic response of the initial structure configuration. The main effect of the smooth impact energy absorption during 15 ms is demonstrated. Notably, that the assumed limits (0.20) for plastic distortions (72) are not reached in the adaptive elements (only 40% of the limit is reached, Fig. 16), and therefore, the impact load capacity of the optimally designed adaptive structure can be still increased. Therefore, a 250% increment of the impact load energy can still be absorbed by the discussed adaptive structure. Because of the symmetry of the structural geometry, it is obvious that, for the second

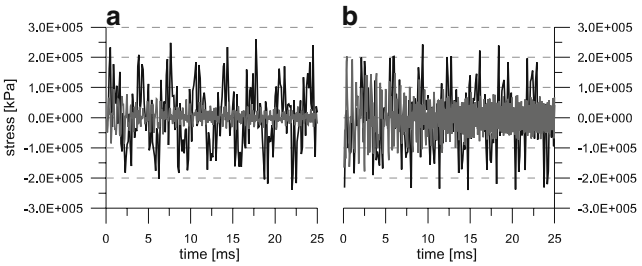

Fig. 19 Development of stresses in maximally loaded elements **a** No. 3, **b** No. 4. (adaptive structure Fig. 15)

impact scenario (masses m2 and m1 impacting nodes 1 and 2, respectively), the optimal yield stress levels will be modified to: σ_I^*=3.6 MPa σ_{II}^*=2.8 MPa.

6 Comments on the problem of optimal design of adaptive structures exposed to multiple impact loads

The VDM-based techniques for fast structural dynamic reanalysis have been developed in the first part of this paper presenting new algorithms for the simulation of structural modifications (coupled modifications of stiffness and mass distribution). Having these algorithms implemented, the problem of optimal remodelling for structures exposed to several possible impact loads has been formulated and solved. The assumed objective function selects, via the gradient-based optimization process, the stiffest structure with material concentrated in the overloaded elements. This resulting structural geometry, with modified topology after the elimination of several elements, forms a basis (in the second part of this paper) for the design of optimally adapting structures with maximal effectiveness of (randomly generated) impact load absorption. The final result of this approach, presented above on the numerical example of the truss beam structure, demonstrates promising effects of efficient impact energy absorption. The slight residual vibration effect observed in Fig. 17 can still be reduced, allowing active control (in real time) of the yield stress level (Mikulowski and Holnicki-Szulc 2007). It is also worth commenting that the residual plastic-like distortions stored in the structure after the impact reception can be released applying the *vibro-relaxation* technique (Pawlowski and Holnicki-Szulc 2004), which allows a continuous use of the adaptive structure exposed to repetitive impact loads. The vibro-relaxation technique is based on the concept of special opening/locking strategies applied to *structural fuses* in the vibrating structure excited by a shaker.

Note, that the final effect of structural redesign proposed in this paper corresponds to the problem of *optimal design of adaptive structure exposed to impact multiloads* determined by the following one-step formulation:

$$\max = \frac{a}{n} \sum_{\tilde{i}} \sum_{i} \sigma_i(t) \Delta\beta_i^0(t) l_i A_i \mu_i \tag{73}$$

subject to equations of motion, constitutive relations, and the inequality constraints imposed on the stress limits (71) and total plastic-like distortions (stroke of the structural fuse dissipater) (72), where n denotes the number of applied structural fuses, a is a scaling parameter to be determined via the numerical practice, and the control parameters are n and $\sigma_i^\star$. The scaling parameters a used in the objective function (73) allow more precisely taking into account the influence of the cost of structural fuse application on the final result of structural design. The assumed on-line dynamic load observability, able to identify the impact (e.g., the dropping mass and its velocity) in a few milliseconds, is a challenging problem, crucial for the *adaptive impact absorption*. Current research, e.g., Sekua et al. (2006), shows that this concept is feasible at least for some applications.

Another issue (not discussed in this paper) deals with the distinction between so-called *fast dynamics* and *slow dynamics* determined through the proportion between the impact velocity and the impacting mass. The same impact energy can be transmitted to the structure by a small dropping mass moving with high velocity and by a heavy mass moving with small velocity. The structural response will be qualitatively different in both cases. Also, the optimal remodelling process discussed in the first part of this paper will lead to different mass redistributions. Therefore, defining the set of admissible impact loads, it is important to determine various possible impact locations, as well as various possible impact "*speeds*" (e.g., proportion of the impacting mass to the square of impact velocity). The corresponding effect to the overall impact absorption demonstrated in the previous section (Fig. 17) is a significant increase of the structural impact capacity (within the same proportion of the impacting mass to the square of impact velocity). However, because of large strokes of the structural fuses, geometrical nonlinearity should be taken into account to get a more precise structural response in the case of higher impact intensities.

Acknowledgements The authors gratefully acknowledge the financial support by the State Committee for Scientific Research in Poland through the projects IN-MAT (PBZ-KBN-115/T08 2008) and INTEGRA **(**R10 005 02**)**. Parts of this paper will be used in the coming book *Smart Technologies for Safety Engineering*, which will be published by John Wiley & Sons in 2008.

References

Holnicki-Szulc J, Pawlowski P, Wiklo M (2003) High-performance impact absorbing materials—the concept, design tools and applications. Smart Mater Struct (12): 461–467

Kolakowski P, Wiklo M, Holnicki-Szulc J (2007) The virtual distortion method (VDM) a versatile reanalysis tool for

structures and systems modifications. Int J Struct Optim doi:10.1007/s00158-007-0158-7

Mikulowski GM, Holnicki-Szulc J (2007) Adaptive landing gear concept—feedback control validation. Smart Mater Struct 16:2146–2158. doi:10.1088/0964-1726/16/6/017

Pawlowski P, Holnicki-Szulc J (2004) Adaptive structures under extreme loads—impact detection, self-adaptation, self-repairing. In: Third European conference on structural control, 3ECSC, Vienna, 12–15 July 2004

Sekua K, Mikulowski G, Holnicki J (2006) Real time dynamic mass identification. In: Structural health monitoring - third European workshop, Grenada, 5–6 July 2006

Simo JC, Huges TJR (1998) Computational inelasticity. Springer, Berlin Heidelberg New York

Wiklo M, Holnicki-Szulc J (2008) Optimal design of adaptive structures, part I. Remodeling for impact reception. Int J Struct Optim (in press)